Physicochemical changes in intermediate-moisture protein bars made with whey protein or calcium caseinate

Short title: Physicochemical changes in whey or caseinate protein bars

Simon M. Loveday, Jason P. Hindmarsh, Lawrence K. Creamer, Harjinder Singh*

Riddet Institute, Massey University, Private Bag 11 222, Palmerston North, New Zealand

* Corresponding author. Tel.: +64 6 350 4401; fax: +64 6 350 5655.

 E-mail address: h.singh@massey.ac.nz (H. Singh).

Abstract

This study examined model protein bars made with whey protein isolate (WPI) or calcium caseinate and stored at 20 °C for 50 days. WPI bars remained very soft and, throughout storage, confocal micrographs showed a continuous matrix containing soluble protein and increasing quantities of glucose crystals. In contrast, calcium caseinate bars had a firm texture within 1–5 days of manufacture (fracture stress 199 ± 16 Pa) and hardened progressively during storage (final fracture stress 301 ± 18 Pa). Electrophoresis showed no evidence of covalent protein aggregation, but there were substantial changes in microstructure over the first day of storage, resulting in segregation of a protein phase from a water–glucose–glycerol phase. Proton nuclear magnetic resonance (^{1}H-NMR) relaxometry and nuclear Overhauser effect spectroscopy (NOESY) experiments showed that water migration away from protein towards glucose and glycerol occurred 10–18 h after manufacture, lowering the molecular mobility of protein. Phase separation was probably driven by the high osmotic pressure generated by the glucose and glycerol. These results confirm that the hardening of protein bars is driven by migration of water from protein to glucose and glycerol, and microstructural phase separation of aggregated protein.

Keywords

Introduction

Intermediate-moisture foods have water activity (a_w) in the region 0.9–0.6 (Roos, 2001, p. 5), and high-protein snack bars (protein bars) fall within this region. The shelf life of intermediate-moisture foods is often limited by Maillard reactions (also known as nonenzymic browning reactions) between carbonyl groups on reducing carbohydrates and exterior amine groups on proteins. Maillard reactions can lead to unappealing color, texture, or flavor, and can seriously affect nutritional value.

As well as Maillard chemical reactions, physicochemical reactions can occur in multicomponent processed foods such as protein bars; these are often far from thermodynamic equilibrium (Mezzenga, 2007). Thermodynamic incompatibility of biopolymers (Tolstoguzov, 2003) and the existence of chemically heterogeneous micro-environments within foods (Kou, Ross, & Taub, 2002) can drive physicochemical reactions during storage. By judicious choice of ingredients and processing conditions, food manufacturers can deliberately create kinetically-limited conditions, such as glassy domains, in order to prolong the shelf life of foods.

The shelf life of protein bars is often limited by their tendency to become unacceptably hard during storage. In an earlier paper (Loveday, Hindmarsh, Creamer, & Singh, 2009), we discussed the occurrence of Maillard reactions and physicochemical reactions in protein bars during storage, as well as current approaches to mitigate hardening and extend shelf life.

In our earlier work with model protein bars containing milk protein concentrate (MPC), hardening did not correspond with changes in protein molecular weight or chemically available amine content (Loveday et al., 2009). Over the first 24 h after manufacture, the microstructure of MPC bars underwent a phase separation, concomitant with the transformation from a liquid batter to a solid bar. Subsequently, there were ongoing changes in the molecular mobility of glucose, glycerol, and water that suggested that the glucose was crystallizing.

This study investigated the effect of protein characteristics on bar hardening, by contrasting the physical and chemical changes in bars made with whey protein isolate (WPI) to those in bars made with calcium caseinate. WPI contains 90% whey protein, some of which is aggregated into dimers, trimers, etc. via disulfide bonding, but the aggregates are still small enough to be soluble. In contrast, calcium caseinate contains calcium-induced aggregates that are much larger and with lower solubility. As the methods and materials were very similar to those in the previous study with MPC, the findings are directly comparable.

Materials and methods

Materials, equipment, and protocols were identical to those described earlier (Loveday et al., 2009) with the exception of the proteins used and some proton nuclear magnetic resonance (^{1}H-NMR) protocols. Some experimental details are omitted here, but can be found in the earlier work.

Bar ingredients

Calcium caseinate (ALANATE^{TM} 385, typical analysis 92.1% protein, 3.9% moisture, 1.5% fat, 0.1% lactose) and WPI (ALACEN^{TM} 895, typical analysis 91.2% protein, 4.6% moisture, 0.3% fat, 0.7% lactose) were supplied by Fonterra Co-operative Group Limited, Auckland, New Zealand.

Product manufacture

Bar material was made in 1 kg batches, consisting of 40% w/w glucose, 20% w/w protein powder, 15% w/w glycerol, 15% w/w water, and 10% w/w cocoa butter. The ingredients were mixed at room temperature (approximately 20ºC) with a Kenwood mixer (Kenwood Corporation, Long Beach, CA) fitted with a flat K-bar type blade. The mixing protocol and the preparation of subsamples were as previously described. Calcium caseinate bars had a_w of 0.65 immediately after manufacture, and a_w for fresh WPI bars was 0.68.

Texture analysis

A lubricated uniaxial compression test was adapted from methods described previously (Watkinson & Jackson, 1999; Watkinson et al., 1997, 2001). A cylindrical core of protein bar material was placed upright on a lubricated Teflon plate and then compressed vertically with a parallel lubricated Teflon plate attached to a TA.HD texture analyzer, equipped with a 500 N load cell (Stable Micro Systems, Godalming, UK) and driven by Texture Expert Exceed software (version 2.64, Stable Micro Systems). Samples were compressed to 80% Cauchy strain at a crosshead speed of 0.83 mm/s.

Force–distance–time data were converted into stress and Hencky strain, and the fracture stress was approximated by the local maximum in stress.

Confocal laser scanning microscopy

During manufacture of the protein bars, a subsample was withdrawn after the final mixing and a few drops of dye were added. The dye was a mixture of Nile Blue (lipid stain) and Fast Green FCF (protein stain) dissolved at 0.2% w/v in a commercial antifading mountant medium, Citifluor (Citifluor Ltd, Leicester, UK). A drop of the mixture was placed on a glass cavity slide and a coverslip was applied. The slides were stored at 20 °C. For one slide of WPI bar material, the coverslip was taped down and the slide was stored upside down.

The slides were examined with a Leica model TCS SP5 DM6000B confocal laser scanning microscope (Leica Microsystems, Wetzlar, Germany), initially approximately 30 min after the completion of mixing and then again the next day, approximately 24 h later, and after 4 and 18 days.

The images were processed with Adobe Photoshop CS version 8.0 (Adobe Systems Incorporated, San Jose, CA) and ImageJ 1.38x (National Institutes of Health, USA; http://rsb.info.nih.gov/ij/). Some images were processed with the built-in fast Fourier transform filter plug-in.

Proton Nuclear magnetic resonance (^{1}H-NMR)

All *^{1}H*-NMR experiments were undertaken in a Bruker (Rheinstetten, Germany) AMX 200 MHz horizontal wide-bore magnet. The proton transverse (or spin–spin) relaxation was measured using the Carr Purcell Meiboom Gill (CPMG) spin−echo pulse sequence (Callaghan, 1991). The major components of the bar material – water, lipid, and polyhydroxy compounds (PHCs) – could be analyzed separately via their representative peaks in the proton NMR spectrum. The major PHCs, glucose and glycerol, could not be separated, as both appear at the −OH position in the proton spectrum. An example spectrum of protein bar material is shown in Loveday et al. (2009).

The transverse relaxation signal of each component was well-fitted in all cases by a bi-exponential model (Schuck, Davenel, Mariette, Briard, Méjean, & Piot., 2002):

$$S = A\exp\left(\frac{t}{T_{2,FAST}}\right) + B\exp\left(\frac{t}{T_{2,SLOW}}\right) \quad (1)$$

$T_{2,FAST}$ and $T_{2,SLOW}$ are the transverse relaxation rate constants of fast- and slow-relaxing protons of each compound, respectively. The values *A* and *B* are the proportions of each component. The T_2 of a compound is related to its molecular mobility and molecular interactions (Lin *et al.*, 2006). As the molecular mobility decreases and/or the level of molecular interactions increases, T_2 will decrease.

The standard Bruker phase-sensitive nuclear Overhauser effect (NOE) pulse sequence (NOESYPH) was used to acquire a two-dimensional nuclear Overhauser effect spectroscopy (2D NOESY) data set with a mixing time (τ_m) of 200 ms. In 2D NOESY, the NOEs appear as cross-peaks, indicating transfer of spin polarization from one spin population to another (cross-relaxation). NOEs can occur between adjacent nuclei within a molecule and/or between nuclei in different molecules. An NOE occurs when two nuclei are close in space (within 5 Å) (Otting & Liepinsh, 1995). The intensity of the NOE peak is proportional to the spin exchange rate and is inversely proportional to the distance between the nuclei.

The forward ($k + 1$) and backward ($k − 1$) magnetization exchange rates between water and PHCs can be calculated using the method described by Zolnai, Juranic, Vikic-Topic, and Macura (2000). The magnetization exchange rate is generally proportional to the chemical exchange rate (in this case, the proton exchange rate between water and PHCs). This method requires two 2D NOESY experiments to be acquired with mixing times τ_m of 0 and 200 ms. The standard Bruker phase-sensitive NOE pulse sequence NOESEYPH was used.

Protein extraction and sodium dodecyl sulfate polyacrylamide gel electrophoresis (SDS-PAGE)

After storage for 1–50 days at 20 °C, samples of bar material were frozen in liquid nitrogen, ground to a fine powder, lyophilized, and stored at −20 °C. Protein extraction and SDS-PAGE followed the procedure of Loveday et al. (2009).

Chemically available amine

The protein bar extracts prepared for SDS-PAGE were also assayed for chemically available amine content. In a 1.5 mL acrylic cuvette (path length 10 mm), 50 μL of extract was added to 950 μL of reagent (Goodno, Swaisgood, & Catignani, 1981). The reader is referred to Loveday et al. (2009) for details of reagent preparation. The cuvette was covered and inverted several times. After incubation at 20 °C for 5 min, the absorbance at 335 nm was measured.

Results and discussion

Texture changes

Protein bars made with WPI were never firm enough for texture analysis, but calcium caseinate bars became very firm during storage (Fig. 1). Two trials were conducted to examine hardening over the first 4 days (trial 1) and longer term hardening during storage for up to 50 days (trial 2).

The hardening process can be delineated into two stages: stage one, an initial 'setting up' during the first 1–5 days, and then a subsequent further hardening over a longer period in stage two. Stage one consisted of a sharp initial increase in fracture stress from 199 ± 16 to 269 ± 21 Pa after 5 days; during stage two, the fracture stress increased at a slower rate to 301 ± 18 Pa after 50 days of storage. This was markedly different from the pattern of hardening with MPC bars (Loveday et al., 2009), where a sharp initial increase was not observed. With MPC bars, the fracture stress was 20.1 ± 1.8 Pa on day 1 and increased at a slightly slower rate to 201 ± 75 Pa on day 50.

Microstructure changes

The microstructures of protein bars made with WPI and calcium caseinate were quite different from the start.

In WPI bar material immediately after manufacture (Fig. 2A), a continuous background of Fast Green staining and a very small number of undissolved powder particles indicated that protein was almost completely dissolved. Within the continuous phase, there were unstained spheres 40–90 μm in diameter (labeled 'a'), presumed to be air bubbles. Lipid was present in rounded droplets up to 75 μm long ('b'), sometimes located at the surface of air bubbles ('c').

Calcium caseinate bar material also had a continuous background of Fast Green staining immediately after manufacture (Fig. 3A). Within the continuous proteinaceous phase, there were particles with irregular shapes that were lightly stained at the surface with Nile Blue (labeled 'a'). As their shapes were reminiscent of other dried dairy powder particles (McKenna, Lloyd, Munro, & Singh, 1999; Nijdam & Langrish, 2006), they were probably undissolved powder particles. Highly spherical particles with unstained centres ('b') were thought to be air bubbles, and the strong Nile Blue staining of rounded particles ('c') sometimes located at the surface of powder particles indicated that they were lipid dropletss.

In fresh calcium caseinate bar material, the background staining was so strong that it was difficult to appreciate the three-dimensional shapes of particles that were stained with Nile Blue or unstained. A clearer picture emerged when the Nile Blue signal from a stack of images taken at different depths was projected at maximum intensity and background noise was reduced with a fast Fourier transform filter (Fig. 3B). The Nile Blue dye lightly stained the surface of protein particles, and their convoluted concave surfaces were evident in the projected signal (labeled 'a'). The highly spherical shape of air bubbles was confirmed ('b'), and the irregular rounded structures that were strongly stained with Nile Blue ('c') were thought to be lipids.

After storing the slide containing WPI bar material for 1 day (24 h) at 20 °C, there was a lot of lipid material and many air bubbles close to the coverslip, which strongly attenuated the lasers. The quality of images from below the surface layer was poor because of signal attenuation. Another slide had been prepared in the same way as the first but was stored with the coverslip side down. Lipid and air bubbles accumulated at the surface opposite the coverslip, and it was possible to obtain high-quality images of the layers nearest the coverslip.

The surface of the bar material closest to the coverslip was depleted of lipid and air bubbles because the slide was stored upside down, and this was reflected in micrographs taken on days 1, 4, and 18 (Fig. 2B, 2C, and 2D).

After 24 h of storage (Fig. 2B), there was still a continuous proteinaceous phase in WPI bar material, indicated by the background of Fast Green staining. Within the continuous phase, there were air bubbles and lipid bodies, but also clusters of unstained elongated 'spiky' structures 10−100 μm long (labeled 'd'). Water−glucose−glycerol 'syrup' is supersaturated with glucose, and these spiky structures were likely to be glucose crystals. After 4 days (Fig. 2C) and 18 days (Fig. 2D) at 20 °C, there were many large crystals taking up much of the continuous phase.

In calcium caseinate bars, the continuous proteinaceous background had disappeared after 24 h (Fig. 3C). Undissolved protein powder particles assumed a more compact network-like structure penetrated by large unstained voids ('d'), which probably contained water, glucose, and glycerol. At higher magnification, the Fast Green signal showed that the powder particles were mostly ovoid with a 'wrinkled' or 'dented' surface (Fig. 3D).

The bar material was more optically dense after 24 h, and the Nile Blue signal was quite weak. Lipid inclusions were present in the protein particle network ('c') and there was some co-localization of the Nile Blue and Fast Green signals ('e'), probably an artifact of amplifying a very weak Nile Blue signal.

The microstructural changes of calcium caseinate bars over the first day were very similar to those seen in protein bars made with MPC (Loveday et al., 2009). In both cases, the continuous background disappeared and the particles assumed a more compact structure. This was not surprising considering that approximately 80% of the protein in MPC consists of caseins.

After 4 days at 20 °C, the protein particles in the calcium caseinate bar material were again clustered (Fig. 3E) around unstained regions. The Nile Blue signal showed what appeared to be clusters of unstained spiky structures (probably glucose crystals) silhouetted against lipid-rich regions ('f'). A very similar microstructure was seen after 18 days (Fig. 3F).

Molecular mobility

Fig. 4 shows the proton relaxation rate constants of the fast-relaxing ($T_{2,FAST}$) components of water and PHCs in WPI or calcium caseinate protein bars stored at 20 °C. It shows that the water and PHC molecules in WPI bars underwent no detectable changes in molecular mobility during storage ($T_{2,FAST}$ was constant). However, with caseinate bars, the mobility of the water and PHCs decreased substantially after the first day of storage and then declined gradually thereafter during storage. This pattern was inverse to the observed changes in the fracture stress (Fig. 1). Thus, calcium caseinate bar hardening could be related to physicochemical changes occurring with the water and PHC components of the bar.

The smaller magnitude of $T_{2,FAST}$ of the water and PHCs in WPI bars is indicative of water and PHCs being associated with a large macromolecule such as protein. This implies that whey proteins undergo little change in hydration levels during storage.

Approximately 70% of the PHC protons and 85% of the water protons in WPI bars were in the fast-relaxing state, compared with 25% of PHC and water protons in caseinate bars. These proportions, and the magnitude of $T_{2,SLOW}$, were approximately constant throughout storage.

Spin interactions

From NOE measurements, it was observed that water in WPI protein bars showed strong interactions with protein and PHCs (Fig. 5A), but water in calcium caseinate bars displayed only very weak interactions with PHCs and no detectable interaction with protein (Fig. 5B). These interactions are probably responsible for the short $T_{2,FAST}$ of water and PHCs in WPI bars (Fig. 4.). The water−PHC NOE in WPI bars was moderately strong on the day after manufacture, and then decreased and increased again during storage to near the original level.

In calcium caseinate bars, the water−PHC NOE was quite indistinct after day 1, and its position fluctuated slightly with storage time. There was no measurable water−lipid NOE with either protein, indicating that the lipids were immiscible in the aqueous phase. Protein-lipid, protein-PHC and lipid-PHC interactions were very weak throughout storage.

The water−protein and water−PHC NOEs in WPI bars are consistent with the interpretation that the background proteinaceous phase in the confocal micrographs (Fig. 2) also contained water and PHCs. The lack of water−protein interactions in calcium caseinate bars was also consistent with the phase separation seen in the micrographs (Fig. 3). It probably resulted from much of the protein being in undissolved particles, and the water being in the unstained areas segregated from the protein particle network.

In calcium caseinate bars, there was clearly considerable change in texture, microstructure, and molecular mobility during the first 24 h after manufacture. In a subsequent experiment, changes in molecular mobility and spin interactions during this time were monitored more closely (Fig. 6).

For the rate of magnetization exchange between water and PHCs, it was possible to separate the forward (water to PHC) and backward (PHC to water) exchange rate constants, k_1 and k_{-1}, respectively, and these are shown in Fig. 6A. From 10 to 18 h after manufacture, k_1 and k_{-1} began to increase, but k_{-1} increased consistently more than k_1, which indicates that a nonequilibrium condition had been set up between the water and the PHCs. The fact that the magnitude of backward exchange (k_{-1}) was greater than the magnitude of forward exchange (k_1) indicated an increase in the population of water molecules that had the potential to exchange with PHCs. In other words, water migrated towards PHCs.

The protein−water NOE (Fig. 6B) decreased during the first 12 h and was approximately constant thereafter. This could indicate either a spatial separation of water and protein or a decrease in the rate of exchange. The $T_{2,FAST}$ of protein did not show a consistent decrease until after 8 h, when it dropped sharply (Fig. 6C).

These data suggest a segregation into one phase rich in protein and a second phase rich in water and PHCs. This was probably driven by osmotic dehydration of protein by the concentrated solution of glucose and glycerol.

Protein modifications

During storage, the chemically available amine fell 33% in WPI bars and 58% in calcium caseinate bars (Fig. 7). In calcium caseinate bars, the rate of decrease in chemically available amine was slightly faster in the first 12 days than subsequently; in WPI bars, there was a plateau at 12−26 days. In MPC bars, chemically available amine fell 38% in the first 12 days and was approximately constant thereafter (Loveday et al., 2009).

Lysine groups in WPI may be protected from glycosylation within the interior of native protein structures or aggregates, whereas the relatively open tertiary structure of caseins

would allow for good access by glucose molecules. The color of WPI bar samples darkened slightly during storage, indicating the onset of 'final stage' Maillard reactions (Hodge, 1953).

The only effect of storage time on SDS-PAGE patterns was a slight blurring of the α_{s2}-casein band for the calcium caseinate bars (data not shown). Similar blurring of this band was seen with MPC bar proteins (Loveday et al., 2009), and was attributed to the addition of one to several glucose molecules at lysine residues, which produced a range of protein–glucose complexes with slightly increased molecular weight.

The loss of chemically available amine did not result in protein cross-linking or large changes in molecular weight, suggesting that reactions were limited to the addition of glucose molecules.

Conclusions

Texture change in calcium caseinate bars during storage followed a different pattern from that seen with MPC bars (Loveday et al., 2009). The main difference in composition is that approximately 20% w/w of the protein in MPC is whey protein, whereas whey proteins are largely absent from calcium caseinate. The presence of whey proteins appears to plasticize the bar matrix, but whey proteins alone (the WPI bars) will not produce a cohesive texture.

Microstructural phase separation occurred in calcium caseinate bars during the first 24 h after manufacture, concomitant with the transformation from a viscous batter to a firm, cohesive solid. The molecular mobility of calcium caseinate proteins fell substantially between day 1 and day 5, perhaps as a consequence of the phase separation. Confocal microscopy and ^{1}H-NMR pointed to glucose crystallization during subsequent storage. This may have accounted for some hardening, but the early microstructural phase separation appeared to be responsible for the most dramatic texture change.

During the first 26 h after manufacture of calcium caseinate bars, there were nonequilibrium interactions among water, protein, and PHCs. There appeared to be a progressive segregation between one phase rich in protein and a second phase rich in water and PHCs. This occurred over the first 18 h after manufacture, probably as a result of water migration away from protein towards PHCs.

This study reinforces earlier conclusions that hardening of protein bars during storage is not caused by chemical cross-linking of proteins. A more important process is the reorganization of the microstructure, driven by osmotic pressure differences and resulting in a segregation of protein from water and PHCs. The aggregation state of proteins affects their solubility and microstructural role in protein bars, and therefore has a large effect on hardness immediately after manufacture and during subsequent storage.

Abbreviations

a_w, Water activity; 2D NOESY, two-dimensional nuclear Overhauser effect spectroscopy; CPMG; Carr Purcell Meiboom Gill; MPC, milk protein concentrate; ^{1}H-NMR, nuclear magnetic resonance; NOE, nuclear Overhauser effect; PHC, polyhydroxy compound; SDS-PAGE, sodium dodecyl sulfate polyacrylamide gel electrophoresis; WPI, whey protein isolate.

Acknowledgments

References

Callaghan, P. T. (1991). *Principles of nuclear magnetic resonance microscopy*. Oxford, UK: Clarendon Press.

Goodno, C. C., Swaisgood, H. E., & Catignani, G. L. (1981). A fluorimetric assay for available lysine in proteins. *Analytical Biochemistry*, *115*(1), 203−211.

Hodge, J. E. (1953). Dehydrated foods, chemistry of browning reactions in model systems. *Journal of Agricultural and Food Chemistry*, *1*(15), 928−943.

Kou, Y., Ross, E. W., & Taub, I. A. (2002). Microstructural domains in foods: effect of constituents on the dynamics of water in dough, as studied by magnetic resonance spectroscopy. In H. Levine, *Amorphous food and pharmaceutical systems* (pp. 48−58). Cambridge: Royal Society of Chemistry.

Lin, X., Ruan, R., Chen, P., Chung, M., Ye, X., Yang, T., Doona, C., & Wagner, T. (2006). NMR state diagram concept. *Journal of Food Science*, *71*(9), R136−R145.

Loveday, S. M., Hindmarsh, J. P., Creamer, L. K., & Singh, H. (2009). Physicochemical changes in a model protein bar during storage. *Food Research International*, *42*(7)*,* 789−806.

McKenna, A. B., Lloyd, R. J., Munro, P. A., & Singh, H. (1999). Microstructure of whole milk powder and of insolubles detected by powder functional testing. *Scanning*, *21*(5), 305−315.

Mezzenga, R. (2007). Equilibrium and non-equilibrium structures in complex food systems. *Food Hydrocolloids*, *21*(5−6), 674−682.

Nijdam, J. J., & Langrish, T. A. G. (2006). The effect of surface composition on the functional properties of milk powders. *Journal of Food Engineering*, *77*(4), 919−925.

Otting, G., & Liepinsh, E. (1995). Protein hydration viewed by high-resolution NMR spectroscopy: implications for magnetic resonance image contrast. *Accounts of Chemical Research*, *28*(4), 171−177.

Roos, Y. H. (2001). Water activity and plasticization. In N. A. M. Eskin & D. S. Robinson, *Food shelf life stability: chemical, biochemical, and microbiological changes* (p. 5). Boca Raton, FL: CRC Press.

Schuck, P., Davenel, A., Mariette, F., Briard, V., Méjean, S., & Piot, M. (2002). Rehydration of casein powders: effects of added mineral salts and salt addition methods on water transfer. *International Dairy Journal*, *12*(1), 51−57.

Tolstoguzov, V. (2003). Some thermodynamic considerations in food formulation. *Food Hydrocolloids*, *17*(1), 1−23.

Watkinson, P., Boston, G., Campanella, O., Coker, C., Johnston, K., Luckman, M., & White, N. (1997). Rheological properties and maturation of New Zealand Cheddar cheese. *Lait*, *77*(1), 109−120.

Watkinson, P., Coker, C., Crawford, R., Dodds, C., Johnston, K., McKenna, A., & White, N. (2001). Effect of cheese pH and ripening time on model cheese textural properties and proteolysis. *International Dairy Journal*, *11*(4−7), 455−464.

Watkinson, P., & Jackson, L. F. (1999). New procedure for estimating the modulus of deformability of cheese from uniaxial compression tests. *Journal of Texture Studies*, *30*(5), 563−580.

Zolnai, Z., Juranic, N., Vikic-Topic, D., & Macura, S. (2000). Quantitative determination of magnetization exchange rate constants from a series of two-dimensional exchange NMR spectra. *Journal of Chemical Information and Computer Sciences*, *40*(3), 611−621.

Fig. 1. Fracture stress of calcium caseinate protein bar samples in a lubricated uniaxial compression test. The data points are the mean of three tests and the vertical bars are standard errors.
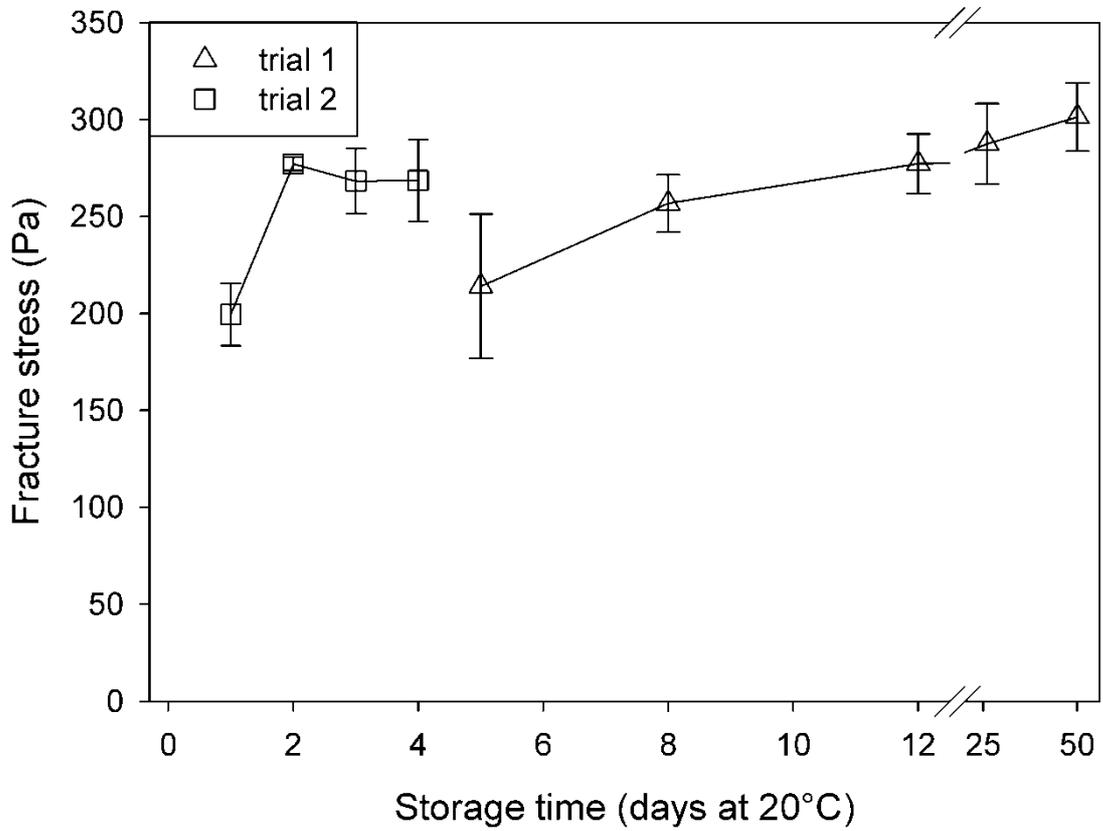
Fig. 2. Confocal micrographs of protein bar material made with WPI. The bar material was examined within 1 h of manufacture (A), or after storage at 20 °C for 1 day (B), 4 days (C), or 18 days (D). Green indicates Fast Green FCF staining (protein) and red indicates Nile Blue staining (lipid).
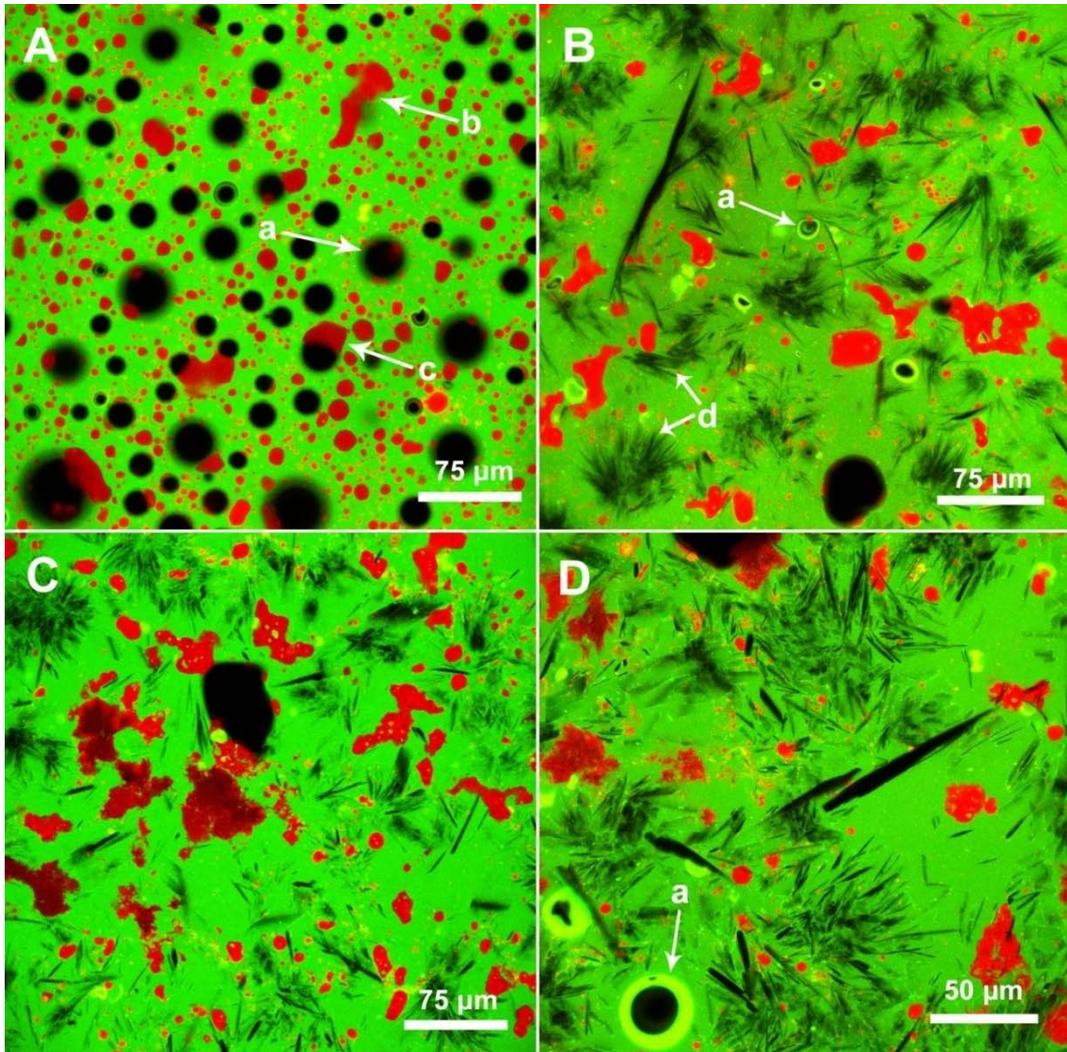
Fig. 3. Confocal micrographs of protein bar material made with calcium caseinate. The bar material was examined within 1 h of manufacture (A, B), or after storage at 20 °C for 1 day (C and D), 4 days (E), or 18 days (F). In A, C, E, and F, green indicates Fast Green FCF staining (protein) and red indicates Nile Blue staining (lipid). B and D show only the Fast Green FCF stain in monochrome; Nile Blue fluorescence was too weak to give a good image.
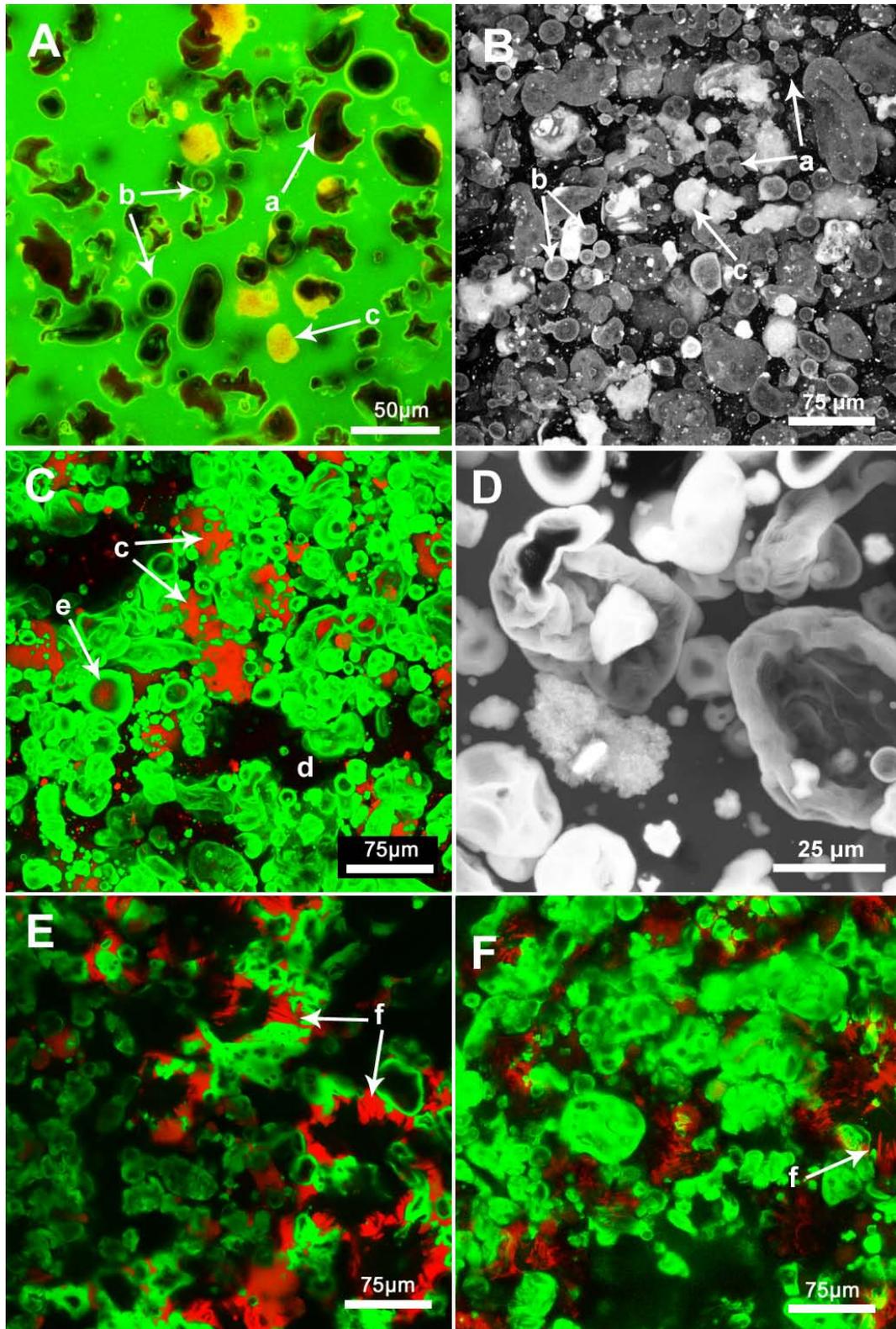
Fig. 4. Proton relaxation rate constants of fast-relaxing ($T_{2,FAST}$) water and PHCs in WPI or calcium caseinate protein bars stored at 20 ºC.
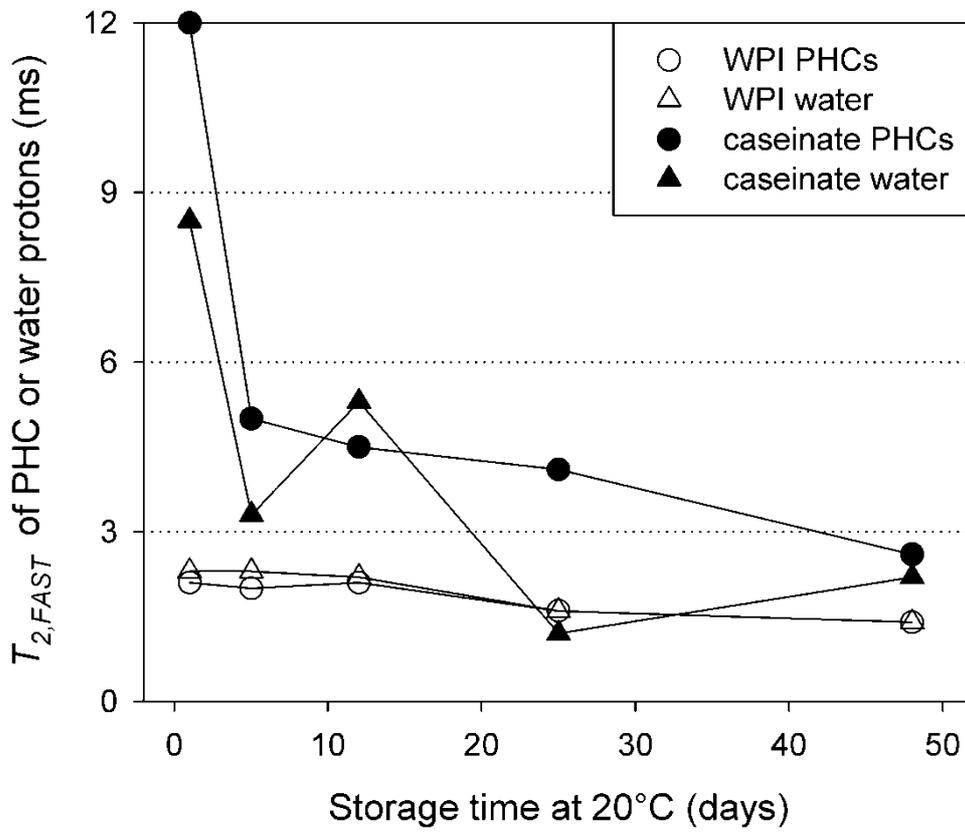
Fig. 5. NOESY spectra of protein bars made with WPI (top) or calcium caseinate (bottom) showing interactions of water with protein and PHCs (glucose and glycerol) during storage at 20 °C.
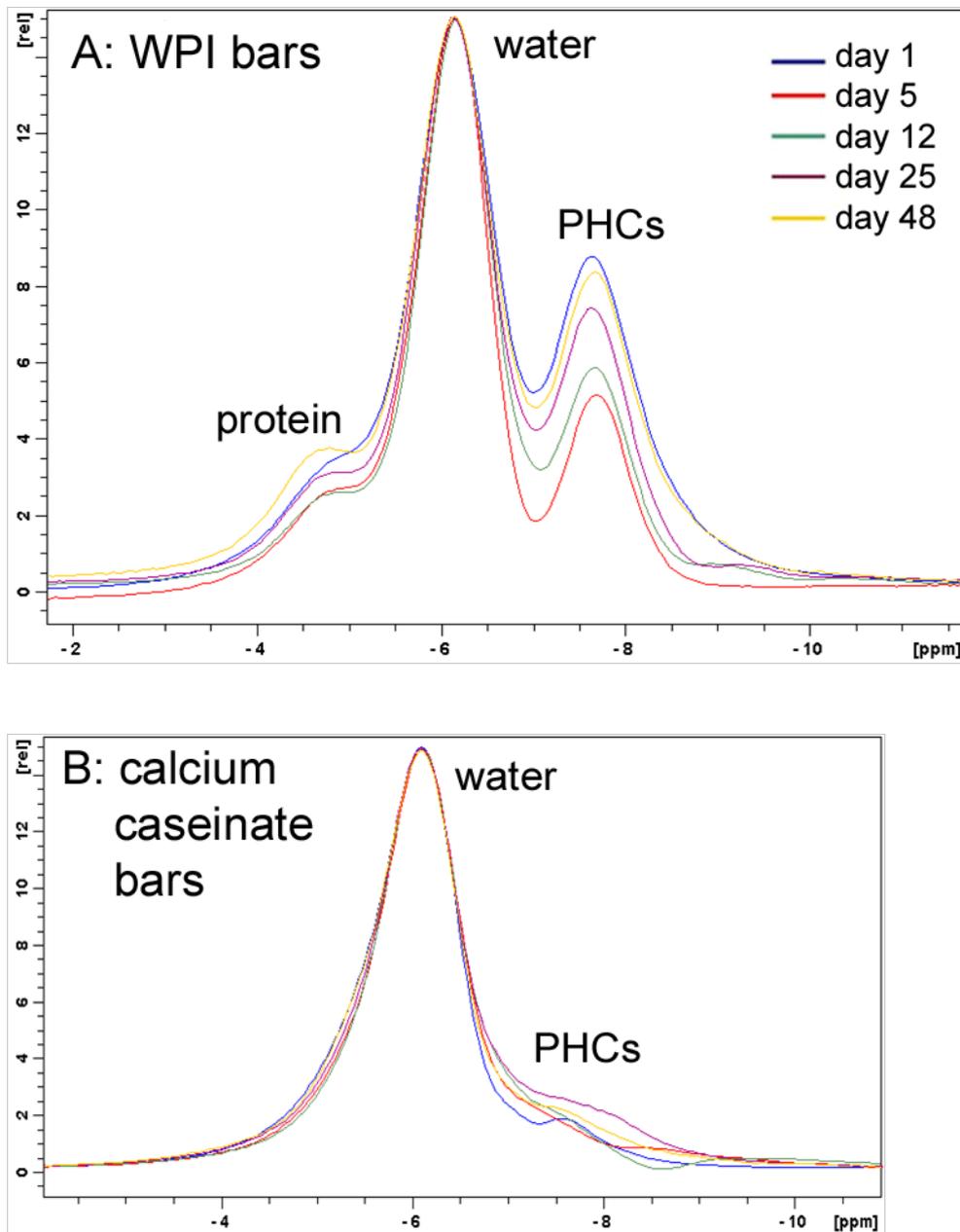
Fig. 6. Molecular mobility and spin interaction (NOE) measurements on calcium caseinate bar material during the first day after manufacture. A: rates of magnetization exchange between water and PHCs. The rate constant k_1 is for water to PHC exchange and the rate constant k_{-1} is for PHC to water exchange. B: Protein−water NOE level. C: Relaxation rate constants of fast-relaxing ($T_{2,FAST}$) water and protein protons.
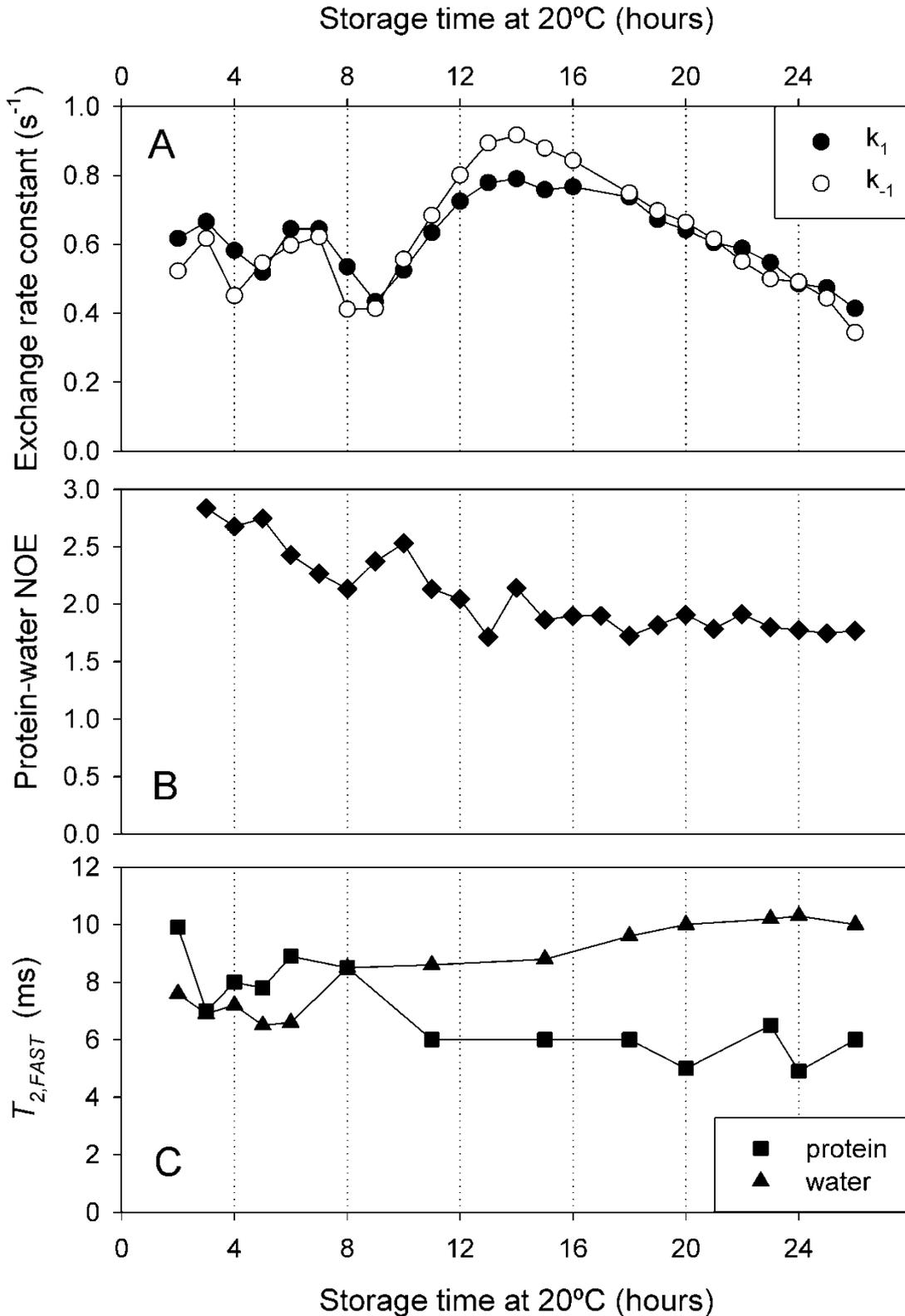
Fig. 7. Absorbance in the chemically available amine assay of extracts from WPI and calcium caseinate protein bars stored at 20 °C for 1–48 days. The vertical bars are the standard errors of triplicates.